

## **NOTICE CONCERNING COPYRIGHT RESTRICTIONS**

This document may contain copyrighted materials. These materials have been made available for use in research, teaching, and private study, but may not be used for any commercial purpose. Users may not otherwise copy, reproduce, retransmit, distribute, publish, commercially exploit or otherwise transfer any material.

The copyright law of the United States (Title 17, United States Code) governs the making of photocopies or other reproductions of copyrighted material.

Under certain conditions specified in the law, libraries and archives are authorized to furnish a photocopy or other reproduction. One of these specific conditions is that the photocopy or reproduction is not to be "used for any purpose other than private study, scholarship, or research." If a user makes a request for, or later uses, a photocopy or reproduction for purposes in excess of "fair use," that user may be liable for copyright infringement.

This institution reserves the right to refuse to accept a copying order if, in its judgment, fulfillment of the order would involve violation of copyright law.

## A PRELIMINARY STUDY OF RELATIVE PERMEABILITY IN GEOTHERMAL ROCKS

Cengiz Satik, Willis Ambusso, Louis M. Castanier and Roland N. Horne

Stanford Geothermal Program  
Stanford University  
Stanford, CA 94305-2220

### ABSTRACT

This paper reports preliminary experimental and numerical efforts towards obtaining steam-water relative permeability and capillary pressure functions under steady-state and adiabatic conditions. In the experimental direction, steady-state nitrogen-water relative permeability experiments were conducted in a Berea sandstone core as a first step. Results obtained from this type of experiment will be compared to those from steam-water relative permeability experiments in order to explore the importance of phase change and heat transfer. Using a high resolution X-ray computer tomography (CT) equipment, saturation distributions along the core were obtained and relative permeabilities for both nitrogen and water were calculated. Preliminary results showed strong end effects for the core length and total flow rate used in the experiment, which therefore suggested either to use of a longer core or to work at a higher total flow rate. Along with the experiment, numerical simulations of simultaneous injection of steam and water into a core were also carried out by using a commercial thermal simulator. At steady-state flow conditions, effects of steam quality and total injection rate on saturation profiles were investigated. Numerical simulation results suggested a core length of 38.10 cm for a flat saturation profile region to exist under typical experimental conditions.

### INTRODUCTION

Reliable measurement of steam-water relative permeability functions is of great importance in geothermal reservoir simulation to match or forecast production performance of geothermal reservoirs. Accordingly, the subject has attracted attention in the past and several experimental and theoretical attempts have been made to study this important problem. In spite of the large number of reported studies, there still remains considerable uncertainty about the exact form of these functions due to the difficulties encountered in the interpretation of results and the lack of under-

standing of microscopic pore-level phenomena such as phase change, heat transfer and capillarity.

Unsteady- or steady-state methods are traditionally used to determine relative permeability. Both methods measure the relative permeabilities as a function of saturation. Unsteady-state methods are based on the Buckley-Leverett (B-L) theory, therefore, they are restricted by its assumptions. These methods have commonly been used for immiscible, isothermal and non-condensing types of displacement processes. Steady-state methods measure relative permeabilities that are independent of time. During steady-state experiments two fluids are injected simultaneously at a known fraction until steady-state conditions are reached. At steady state, relative permeabilities are calculated by using a theory that relies on Darcy's law extended for multi phase flow. The corresponding saturation values should also be determined. The main assumption of these methods is the requirement for existence of a flat saturation profile, which can be achieved by using a sufficiently long core or high flow rates. Otherwise, the *capillary end-effects* commonly observed in many experiments may complicate interpretation of the results.

Steady-state methods have been used to determine steam-water relative permeabilities under adiabatic conditions. Even though such experiments are simpler, previous literature has pointed out major difficulties, particularly in the interpretation of results. Problems have arisen in the determination of accurate saturation profiles and also in the treatment of phase change, heat transfer, capillarity and injection rate. Two typical problems have been studied in the past: one involving an injection of a subcooled liquid which undergoes a phase change inside the porous medium after the injection, and another involving simultaneous injection of steam and water.

An early attempt was reported by Arihara (1974) who was unable to measure saturation directly but calculated it instead. The calculation was performed by first measuring the temperature profile along the core to obtain fluid properties, enthalpy and pressure,

and by using steady-state, single-component, non-isothermal and adiabatic flow equations, combined with a relative permeability ratio and a water-oil permeability vs. saturation curve. Trimble and Menzie (1975) developed relative permeability curves for Boise and Berea sandstone cores. They reported unusually low steam relative permeability. Later on, Chen (1976) made an important advance by measuring water saturation directly using a capacitance probe technique, but he assumed a nearly linear relationship between the capacitance probe signal and the water saturation. Council (1979) used Chen's method to obtain the water saturation for the process of in-situ evaporation of flowing water. He obtained steady-state steam-water relative permeabilities for a synthetic sandstone core under adiabatic conditions. Council (1979) also measured nitrogen-water relative permeabilities and concluded that steam-water relative permeabilities are very different from those of nitrogen-water at high water saturations. His data indicated steam relative permeability being large in all but a narrow region of high water saturation. Later, Monsalve et al. (1984) studied the effects of surfactants on steam-water systems and concluded that relative permeability to water increased with increasing surfactant concentration rather than holding constant. Additionally, Monsalve (1984) observed that steam relative permeability decreased drastically at a certain water saturation, results similar to those of Council (1979). Verma (1986) reported a study of relative permeability for two-phase concurrent flow of steam and water. He compared his results with those from oil/water, gas/water and gas/oil systems. He found out that wetting phase relative permeability curves were in good agreement while steam relative permeability was significantly higher than that of non-wetting phase. Recently, Sanchez (1987) reported steady-state adiabatic steam-water relative permeability experiments for an unconsolidated Ottawa sand pack. Sanchez (1987) measured liquid saturations by analyzing the output of a 10 microliter pulse input of NaCl-36 through an HPLC sample injector. He concluded that steam-water relative permeabilities can be represented accurately by gas-liquid permeability for high permeability reservoirs. Very recently, similar results were also reported by Piquemal (1994) who attempted to determine steam-water relative permeabilities in an unconsolidated sandstone.

The wide discrepancy observed in the previous experimental results suggests that the interpretation of the data may not be correct. Additionally, a major problem of obtaining reliable saturation profiles has been emphasized. Recognizing that saturation and temperature profiles are dependent on parameters such as injection rate and temperature, steam

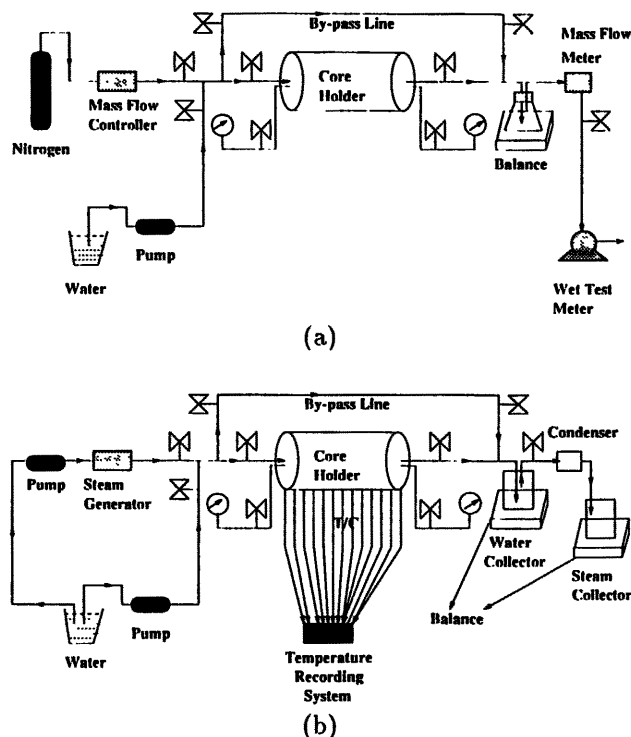


Figure 1: Schematics of experimental apparatus for (a) nitrogen-water and (b) steam-water injection.

quality, system pressure, core permeability and length and also that determining accurate saturation profiles is crucial, we initiated a systematic study to determine steady-state steam-water relative permeabilities directly. With the use of our X-ray computer tomography (CT) scanner equipment, which is capable of producing high-resolution images, we can overcome the difficulty of obtaining accurate saturation distributions along the core samples while multi-phase experiments are being conducted. This paper reports our preliminary results towards the final goal. First, we describe our experimental apparatus and procedure. Next, we discuss some preliminary results from a nitrogen-water injection experiment. Finally, we report some numerical simulation results for the problem of simultaneous injection of steam and water.

## EXPERIMENTAL APPARATUS AND PROCEDURE

The experimental apparatus used for the preliminary nitrogen-water relative permeability measurements is shown in Figure 1a. It consists of a core holder, two pressure transducers, a liquid pump, a mass flow

controller, a mass flow meter, a balance and a wet-test meter. Two pressure taps located at the inlet and outlet ends of the core holder were used to measure the water phase pressure during the experiment. Nitrogen injection and production rates are controlled and monitored with the use of mass flow-controller, flow-meter and wet-test meter while a liquid pump was used to inject water into the core and a balance was used to measure water production rate. However, a different experimental apparatus is required for steam-water relative permeability experiments. A schematic of the tentative experimental design for the steam-water relative permeability experiments is shown in Figure 1b. This design will consist of a core holder, two liquid pumps, a steam generator and steam and water collection systems. Pressures will be measured at the inlet and outlet ends of the core while temperatures will be measured by thermocouples inserted at various locations along the core. Several heat flux sensors will be placed along the length of the core holder to measure heat losses.

During an experiment, the core holder is placed inside the high resolution X-ray computer tomography (CT) equipment in order to obtain in-situ saturation profiles along the core. The principles of the use of X-ray CT are described in Johns et al. (1993). Here, we shall summarize this method briefly. The X-ray CT method, as a nondestructive imaging method, enables us to construct an internal image of an object. Simply, an X-ray source is revolved around the object to take various projections at many angles and the data collected are then used to reconstruct the internal image. As X-ray beam travels through the object, changes in density and/or thickness of the material cause differences in X-ray attenuation. The image data obtained with the scanner are normalized to  $CT$  numbers whose unit is called a Hounsfield.

The experimental procedure as follows. First, air inside the pore space is displaced out by injecting several pore volumes of  $CO_2$  and then the core is scanned at predetermined locations to obtain dry-core  $CT$  ( $CT_{dry}$ ) values. Next, water is injected into the core to remove  $CO_2$  and to eventually saturate it completely. This step continues until the core is completely saturated with water, at which time the core is X-ray scanned again at the same locations to obtain wet-core  $CT$  ( $CT_{wet}$ ) values and, inlet and outlet end pressure readings are taken at this time. Steady-state relative permeability experiments involve injection of varying fractions of nitrogen and water (or steam and water), at a constant total flow rate, into the core. Measurements done at each step result in a single data point on relative permeability vs. saturation curve. Starting from completely water saturated core and inject-

ing nitrogen at increasing fractions will give rise to a drainage process while the opposite procedure gives rise to an imbibition process. Each step continues until steady-state conditions at which injection and production rates become the same for both nitrogen and water and also inlet and outlet end pressures stabilize. At the onset of steady-state conditions, another X-ray scanning is done along the core at the same locations to obtain  $CT$  ( $CT_{exp}$ ) values corresponding to the particular gas-water fraction. To complete the step, inlet and outlet end pressure readings are taken again. Next, the nitrogen-water fraction is changed, keeping total flow rate constant, and the procedure is repeated.

After the experiment is completed, interpretation software is used to calculate the porosity and saturation distributions from the  $CT$  values obtained with the scanner. To calculate porosity the following expression is used:

$$\phi = \frac{CT_{wet} - CT_{dry}}{CT_{water} - CT_{air}} \quad (1)$$

where  $CT_{water}$ ,  $CT_{air}$  are  $CT$  numbers for water and air, respectively. Similarly, the expression used to calculate saturations is:

$$S_g = \frac{CT_{wet} - CT_{exp}}{CT_{wet} - CT_{dry}} \quad (2)$$

and

$$S_w = 1 - S_g \quad (3)$$

where  $S_g$  and  $S_w$  denote gas and water saturations, respectively. Relative permeabilities for water and nitrogen can be calculated by using Darcy's law,

$$k_{rw} = \frac{\mu_w q_w L}{k A \Delta p_w} \quad (4)$$

for water and

$$k_{rg} = \frac{\mu_g q_g L}{k A \Delta p_g} \quad (5)$$

for gas. Here  $k_r$ ,  $\mu$ ,  $q$ ,  $k$ ,  $A$ ,  $L$  and  $\Delta p$  are relative permeability, flow rate, permeability, cross sectional area and length of the core and pressure drop, respectively. Subscripts  $w$  and  $g$  denote water and gas, respectively. In these equations, all of the parameter values are either measured or determined by using the experimental data. For the preliminary experiment, we measured water and gas flow rates and water pressure drop but calculated nitrogen pressure drop by using a nitrogen-water capillary pressure curve.

## PRELIMINARY RESULTS

### EXPERIMENTAL

A preliminary experiment was conducted to measure nitrogen-water relative permeability. The core

used in this experiment was a Berea sandstone, the length and diameter of which were 25.4 cm and 5.08 cm, respectively. The total injection rate of fluids was 12 cc/min. Porosity and saturation distributions, and relative permeability were obtained by using the results of this experiment, as discussed below.

First, the absolute permeability of the core was calculated by using Equation 4 with  $k_{rw} = 1$  and also with the results of the wet-core step. The value was calculated to be 601 mD. Next, the porosity distributions along the core were obtained by inserting the CT values in Equation 1. In Figure 2, we show the porosity distributions at four different locations through the

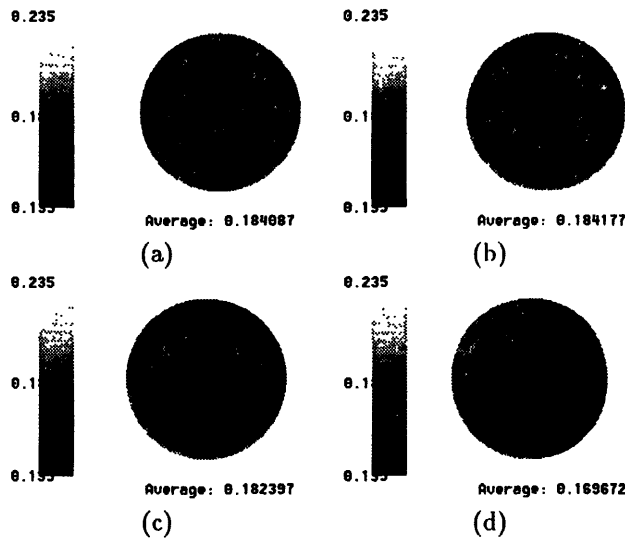


Figure 2: Porosity distributions obtained from X-ray CT scanning at (a) 0.2 cm, (b) 8.2 cm, (c) 16.2 cm and (d) 25.2 cm from the inlet end of the core.

core (at 0.2, 8.2, 16.2 and 25.2 cm from the inlet end of the core). Average porosity was calculated to be 18.50 %. During the experiment, we obtained a total of 26 slices from the X-ray CT scanning. All of those slices indicated a fairly homogenous core with average porosity decreasing slightly (from 18.4087 % to 16.9672 %) towards the outlet.

Saturation distributions were also calculated by using Equations 2a and b. In Figure 3, we show nitrogen saturation distributions at four different locations along the core (0.2, 8.2, 16.2 and 25.2 cm from the inlet end of the core). Nitrogen saturation is higher closer to the inlet and decreases closer towards the outlet. Saturation distributions shown in the figure are consistent with the porosity distributions (Figure 2). Small gas saturations spots observed in Figures 3b, c and d correspond to smaller porosity values, implying

gas (non-wetting) phase residing in large pores with water (wetting) phase residing in smaller pores.

Average water saturation distributions calculated using Equation 2b for four different values of  $f_g$  (gas fraction), defined as the fraction of the gas flow rate to the total flow rate), are shown in Figure 4. All of the saturation distributions shown in the figure indicates very strong inlet end effects (saturations starting from about 60 % at the inlet and increasing with distance) and a possible weak outlet end effect. Flat saturation profiles do not exist probably due to the strong end effects. Moreover, water saturation changes significantly as  $f_g$  increases from 0.16 to 0.3333 although further increase in  $f_g$  (up to 0.84) does not seem to change the saturation levels significantly. These preliminary results suggest either using a longer core or operating at a higher total flow rate to obtain a flatter saturation profile.

A summary of the preliminary experiment is given in Table 1. Water pressure drops were measured directly

Table 1: Summary of preliminary results for a nitrogen-water relative permeability experiment.

$f_g$	$\Delta P_w$ , psi	$\Delta P_g$ , psi	$k_{rw}$	$k_{rg}$
0	5	0	1.0	0.0
0.16	16	20.17	0.312	0.0009
0.33	19	23.50	0.210	0.00155
0.50	15	19.67	0.1999	0.0028
0.67	11	15.67	0.1817	0.0046
0.84	6	10.27	0.1666	0.0089

during the experiment. Gas pressure drops, however, were calculated by using a nitrogen-water capillary pressure curve obtained for Berea sandstone (borrowed from the study of Oak et al. (1990)). Finally, relative permeabilities for each phase were calculated by using Equations 4 and 5. Water relative permeabilities decreases monotonically as  $f_g$  increases while gas relative permeabilities are almost zero. This implies a very sharp increase in the  $f_g$  vs.  $S_g$  curve within a very narrow gas saturation range. Therefore, it is necessary to increase the  $f_g$  value to between 0.84 and 1.0 to have an increase in gas relative permeability.

## NUMERICAL

To investigate the effects of various parameters and to determine a proper core length along which a flat saturation profile may exist, we carried out numerical simulations by using a commercial thermal simulator. Simultaneous injection of steam and water under adiabatic conditions were simulated. In the context of this

Table 2: Typical parameter values used in the numerical simulations.

$\rho_w$	=	960.85	kg/m <sup>3</sup>
$C_{pw}$	=	$4.2092 * 10^3$	J/kg - K
$\lambda_w$	=	0.6808	W/m - K
$\mu_w$	=	$2.4799 * 10^{-4}$	N - s/m <sup>2</sup>
$L_V$	=	$2.2568 * 10^6$	J/kg
$\rho_s$	=	0.5886	kg/m <sup>3</sup>
$C_{ps}$	=	$4.2092 * 10^3$	J/kg - K
$\lambda_s$	=	0.6808	W/m - K
$\mu_s$	=	$2.4799 * 10^{-4}$	N - s/m <sup>2</sup>
$\rho_r$	=	2200.0	kg/m <sup>3</sup>
$C_{pr}$	=	$8.3732 * 10^2$	J/kg - K
$\lambda_r$	=	6.808	W/m - K
$k$	=	400	mD
$\phi$	=	0.20	
$A$	=	$5.08 * 10^{-4}$	m <sup>2</sup>
$L$	=	0.381	m
$P_{init}$	=	$1.0133 * 10^5$	N/m <sup>2</sup>
$T_{init}$	=	294.15	K

paper, we shall discuss only the effects of steam quality and total injection rates. Parameter values used in the simulations are given in Table 2. In the table,  $\rho$ ,  $C_p$ ,  $\lambda$ ,  $L_v$ ,  $p$  and  $T$  denote density, specific heat capacity, thermal conductivity, latent heat of evaporation, pressure and temperature, respectively. Subscripts  $w$ ,  $s$  and  $r$  represent water and steam phases, and rock, respectively.

In Figure 5, we show water saturation, temperature and pressure profiles obtained from numerical simulation for parameter values given in Table 2 and for a total injection rate ( $m_i$ ) of 5 kg/D and a mass steam quality ( $X_s$ ) of 0.25. In order to simulate end effects numerically, the capillary pressure was set to zero and the permeability was assigned a large value of 20000 mD in both the first and last grid blocks. The water saturation profile shows both inlet (an increase in water saturation) and outlet (first an increase or buildup followed by a decrease in water saturation) end effects which are restricted to narrow regions, otherwise a flat saturation profile is observed. To interpret our results, we followed a recent study of Parlar et al. (1990), which showed an analytical attempt to understand the end effects for steady-state, vapor-liquid concurrent flows in porous media. Because capillary pressure is zero at the inlet and outlet ends and is non-zero otherwise steam entering the core condenses at the inlet, causing a sudden temperature drop (Figure 5b). However, towards the outlet end, the effect is the opposite

such that capillary pressure becomes zero from a non-zero value. This will induce first a saturation buildup and then a saturation decrease at the outlet, which are associated with a condensation process followed by an evaporation (see also Parlar et al., 1990). The temperature profile is also consistent with this interpretation. The temperature decreases while condensation occurs and flattens when evaporation takes place (see Figure 5b). The pressure profile shown in Figure 5c follows the trend of the temperature profile since both steam and water phases are flowing under saturated conditions.

Water saturation profiles obtained for five different steam quality values ( $X_s = 0.0005, 0.05, 0.25, 0.50$  and  $0.75$ ) are shown in Figure 6. As steam quality increases greater displacement of water takes place therefore the average water saturation value within the flat region decreases. Figure 6 shows that the flat saturation value is about 0.40 for  $X_s=0.75$  while it is about 0.74 for  $X_s=0.0005$ . As steam quality decreases the flat saturation region becomes narrower.

The effect of total injection rate is shown in Figure 7. Total flow rate has increased from 0.5 kg/D to 10 kg/D while steam quality has been kept as 0.25. The results shown are as expected. The region where outlet end effects are dominant becomes narrower as total flow rate increases since macroscopic capillary number also increases. Finally, we investigated the effect of the core length on saturation profiles. The simulation results suggested that a minimum core length of 38.10 cm would be required to avoid the end effects for typical experimental conditions.

## CONCLUSIONS

Preliminary experimental and numerical efforts were made towards the final goal of determining steam-water relative permeability and capillary pressure functions in geothermal rocks. Experiments with nitrogen and water were carried out as a first step. Porosity and saturation distributions were calculated by using high resolution X-ray computer tomography (CT) equipment. Results indicated strong end effects, suggesting either use of a longer core or operation at higher total flow rates.

Numerical simulations were also carried out by using a commercial thermal simulator to study the problem of simultaneous steam-water injection into a porous medium under adiabatic conditions. Numerical simulation results suggested the minimum core length to maintain a flat saturation profile would be 38.10 cm for typical laboratory conditions. Effects of steam quality and total injection rate were investigated. The results obtained were as expected.

## ACKNOWLEDGEMENTS

This work was supported by DOE contract DE-FG07-90ID12934, the contribution of which is gratefully acknowledged. The authors also would like to thank Aldo Rossi for his assistance. The thermal simulator (STARS) was made available by Computer Modelling Group, Calgary, Alberta.

## REFERENCES

- N. Arihara. 1974. A study of nonisothermal single and two-phase flow through consolidated sandstones. Ph. D. Thesis, Stanford University, Stanford, California.
- K. K. Chen. 1976. Measurement of water content in porous media under geothermal fluid flow conditions. Ph. D. Thesis, Stanford University, Stanford, California.
- J. R. Counsil. 1979. Steam-water relative permeability. Ph. D. Thesis, Stanford University, Stanford, California.
- R. A. Johns, J. S. Steude, L. M. Castanier, and P. V. Roberts. 1993. Nondestructive measurements of fracture aperture in crystalline rock core using x ray computed tomography. *J. Geophys. Res.*, 98(B2):1889-1900.
- A. Monsalve, R. S. Schechter, and W. H. Wade. 1984. Relative permeabilities of surfactant/steam/water systems. Paper SPE 12661 presented at the 1984 SPE Symposium on Enhanced Oil Recovery, Tulsa, April 15-18.
- M. J. Oak, L. E. Baker, and D. C. Thomas. 1990. Three-phase relative permeability of berea sandstone. *J. Petroleum Tech.*, pages 1054-1061.
- M. Parlari, M. Zeybek, and Y. C. Yortsos. 1990. Steady-state, vapor-liquid concurrent flow: relative permeabilities and end effects. Paper SPE 20054 presented at the SPE California Regional Meeting, Ventura, CA, April 4-6.
- J. Piquemal. 1994. Saturated steam relative permeabilities of unconsolidated porous media. *Transport in Porous Media*, 17:105-120.
- J. M. Sanchez. 1987. Surfactant effects on the two-phase flow of steam/water and nitrogen/water in an unconsolidated permeable medium. Ph. D. Thesis,

University of Texas, Austin, Texas.

- A. E. Trimble and D. E. Menzie. 1975. Steam mobility in porous media. Paper SPE 5571 presented at the 50th Annual Fall Meeting, SPE of AIME, Dallas, TX, Sept.
- A. K. Verma. 1986. Effects of phase transformation on steam water relative permeability. Ph. D. Thesis, University of California, Berkeley, CA.

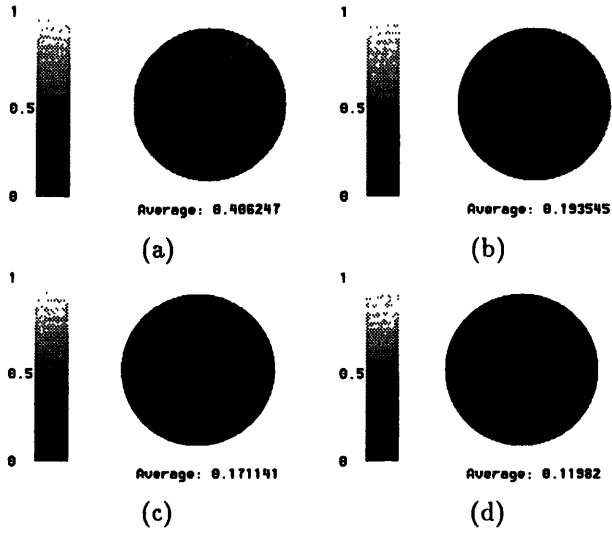


Figure 3: Nitrogen saturation distributions obtained from X-ray CT scanning at (a) 0.2 cm, (b) 8.2 cm, (c) 16.2 cm and (d) 25.2 cm from the inlet end of the core.

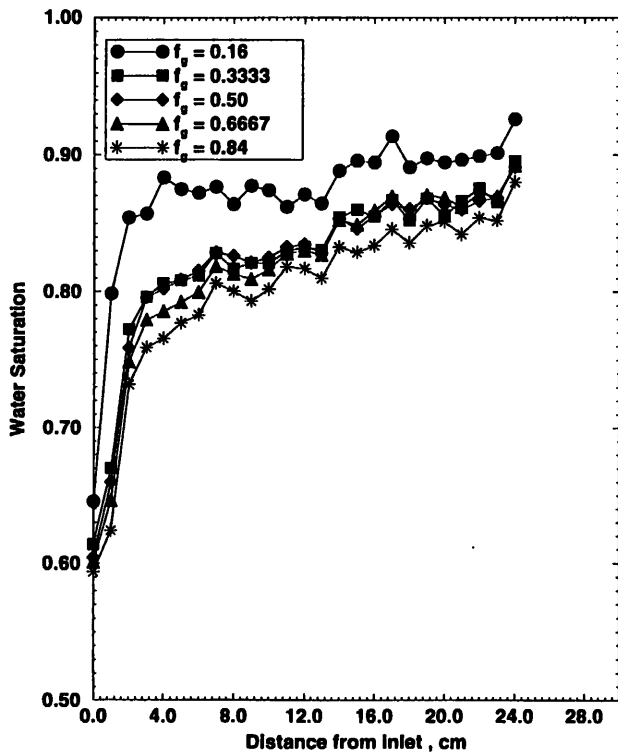
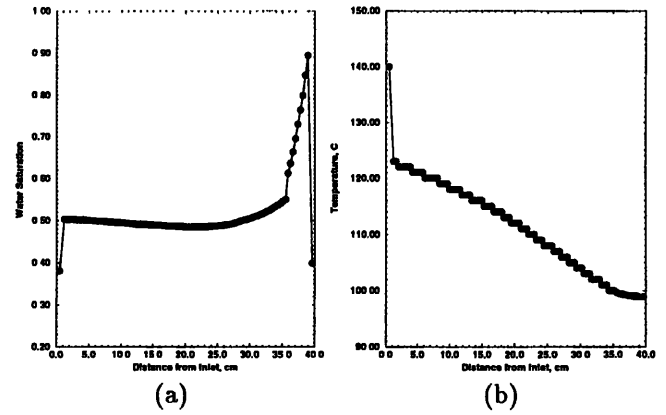


Figure 4: Water saturation distributions obtained in nitrogen-water steady-state experiments.

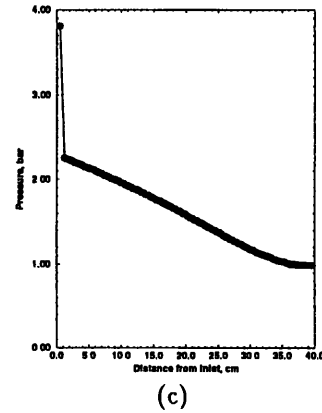


Figure 5: Steady-state steam-water simulation results (a) Saturation, (b) temperature and (c) pressure distributions.

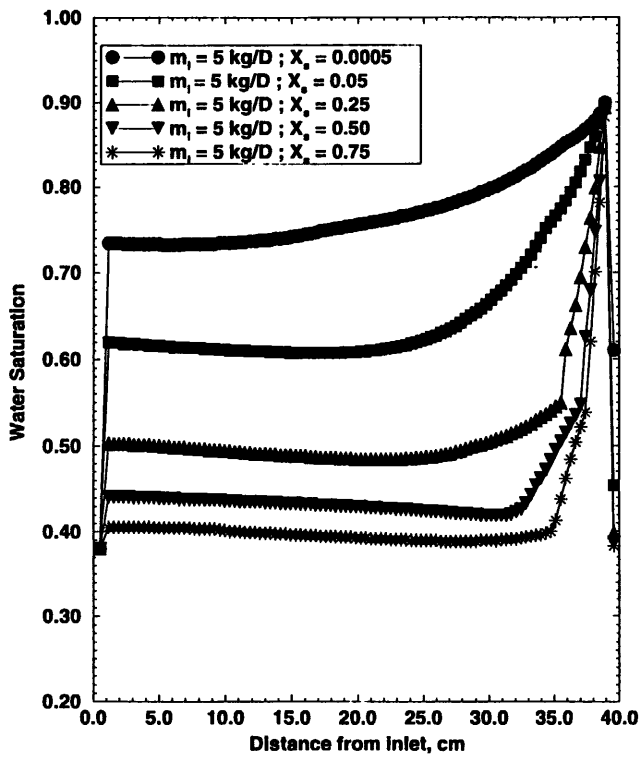


Figure 6: Water saturation distributions obtained in steam-water steady-state simulations at five different steam quality values.

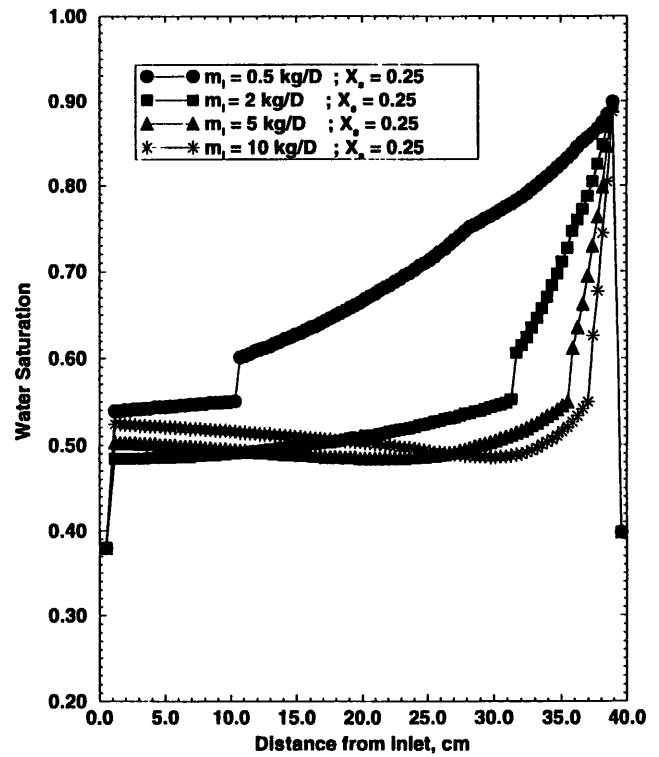


Figure 7: Water saturation distributions obtained in steam-water steady-state simulations at four different total injection rates.